PNAS RESEARCH ARTICLE | NEUROSCIENCE

Trem2 exacerbates ischemic brain injury through Gpnmb in a photothrombotic stroke model

Xuezhen Chen[a,b,c,1], Kunyu Li[a,1], Siyu Liu[a,d,1], Junyi Zhao[a,d,1], Sagun Tiwari[a,e], Fan Zeng[a,b,d], Yue Zhao[a,b,d], Pingping Zhang[f,g], Han Tang[f,g], Hong Zhao[f,g], Helmut Kettenmann[a,b,d,h,2], Xianyuan Xiang[b,d,2], and Xinzhou Zhu[a,b,d,i,2]

Affiliations are included on p. 11.

Edited by Lawrence Steinman, Stanford University Arnold and Mabel Beckman Center for Molecular and Genetic Medicine, Stanford, CA; received August 28, 2025; accepted February 26, 2026

Ischemic stroke is a major public health challenge, with microglia-mediated neuroinflammation exerting both protective and detrimental effects on neuronal survival. The Triggering receptor expressed on myeloid cells 2 (Trem2), predominantly expressed by microglia, has been reported to confer neuroprotection in the middle cerebral artery occlusion (MCAO) model. Paradoxically, in patients, elevated plasma soluble Trem2 (sTrem2) levels correlate with increased risk and poor outcomes. To test the impact of Trem2 function in the context of stroke, we utilized the photothrombotic stroke model which elicited strong Trem2 upregulation, a clinical feature which is not mimicked in MCAO models. Trem2 depletion reduced infarction volume, suppressed proinflammatory cytokine production, preserved neuronal survival, and lessened motor and neurological impairment. Conversely, intracerebral administration of sTrem2 exacerbated neuronal loss, amplified inflammation, and worsened neurological deficits. Integrated mouse-human transcriptomic analyses identified glycoprotein nonmetastatic B (Gpnmb) as a conserved downstream effector of Trem2. Soluble Gpnmb (sGpnmb) administration abolished the protective effects of Trem2 depletion, promoting microglial activation, lipid accumulation, and neuronal damage. Additionally, plasma sTrem2 and sGpnmb levels were elevated in stroke patients, positively correlated, and may serve as biomarkers of poor prognosis. These findings uncover a detrimental role for Trem2 in ischemic stroke, provide mechanistic insight into the link between sTrem2 and poor clinical outcomes, and identify the Trem2–Gpnmb axis as a potential therapeutic target to mitigate poststroke neuroinflammation.

ischemic stroke | photothrombotic model | middle cerebral artery occlusion model | Trem2 | blood biomarker

Significance

Stroke is a leading cause of death and disability, with microglia-driven inflammation as a key contributor to brain injury. The microglial receptor Trem2 has shown inconsistent roles: protective in a classic stroke model but associated with worse outcomes when its soluble form (soluble Triggering receptor expressed on myeloid cells 2) is elevated in patients. Using a photothrombotic mouse model that better mirrors Trem2-mediated responses as observed in patients, we found that Trem2 drives sustained inflammation and exacerbates neuronal deficits. These results emphasize the importance of model selection in studying poststroke neuroinflammation and suggest Trem2 and its downstream pathways as potential therapeutic targets.

Stroke remains a leading cause of death and disability worldwide (1), with thrombolysis and mechanical thrombectomy as the only approved treatments for ischemic stroke (2). Despite advances in acute care, effective therapies to enhance poststroke recovery are lacking. Neuroinflammation is a key feature of postischemic brain, which can be beneficial by clearing debris and supporting tissue remodeling, but can also drive secondary injury and neurological decline (3). Microglia, the resident innate immune cells of the central nervous system, are key regulators of this inflammatory response (4, 5). With high heterogeneity and plasticity (6), they exert phagocytic functions and shape both pro- and anti-inflammatory responses, thereby shaping both beneficial and harmful outcomes (7).

The triggering receptor expressed on myeloid cells 2 (Trem2), a microglia-specific receptor in the brain, has emerged as a crucial regulator of microglial state transitions in neurodegeneration. Genetic variants of Trem2, such as R47H, increase the risk of late-onset Alzheimer's disease (AD) (8, 9). However, the biological consequences of Trem2 signaling are highly context dependent. In amyloid-bearing animals, Trem2 may serve protective functions, by limiting tau accumulation and spreading (10–12), yet its deficiency may also reduce plaque accumulation (13). In tauopathy models, Trem2 deficiency attenuates neuroinflammation and ameliorates tau pathology (14, 15). Adding further complexity, Trem2 is also released as soluble Trem2 (sTrem2) through proteolytic shedding or alternative splicing (16). sTrem2 can modulate microglial activity and has been linked to beneficial effects on tau pathology (17). In AD patients, higher sTrem2 levels in cerebrospinal fluid are associated with slower cognitive decline (18, 19). These findings underscore the context-dependent effects of Trem2 and sTrem2, making model choice decisive for biological interpretation.

The role of Trem2 in ischemic stroke remains ambiguous. Most preclinical studies have been performed in MCAO models, which have frequently concluded that Trem2 is protective, often attributed to enhanced phagocytosis and reduced injury (20, 21)

Author contributions: H.Z., H.K., X.X., and X.Z. designed research; X.C., K.L., S.L., J.Z., S.T., F.Z., Y.Z., P.Z., H.T., and X.Z. performed research; X.C., K.L., S.L., J.Z., P.Z., H.T., X.X., and X.Z. analyzed data; and H.K., X.X., and X.Z. wrote the paper.

The authors declare no competing interest.

This article is a PNAS Direct Submission.

[1]X.C., K.L., X.L., and J.Z. contributed equally to this work.

[2]To whom correspondence may be addressed. Email: kettenmann@mdc-berlin.de, xiang.xy@suat-sz.edu.cn, or xz.zhu@siat.ac.cn.

This article contains supporting information online at https://www.pnas.org/lookup/suppl/doi:10.1073/pnas.2523148123/-/DCSupplemental.

Published April 14, 2026.

(summarized in *SI Appendix*, Table S1). However, the studies use MCAO show considerable heterogeneity in both Trem2 induction and phenotype. Studies using Trem2 knockout (KO) mice (22), siRNA-mediated knockdown, or overexpression strategies report divergent effects on infarction size, inflammation, and neurological outcomes (20, 21, 23–26) (*SI Appendix*, Table S1). Furthermore, Trem2 induction is often minimal in MCAO models, with some reports showing no change in mRNA or serum sTrem2 levels (27, 28). These inconsistencies indicate that the MCAO model may be insufficient to accurately assess the role of Trem2, potentially underestimating its contribution to poststroke inflammatory responses.

In contrast, clinical data show that elevated plasma sTrem2 correlates with worse outcomes (29, 30), impaired cognition (31), and higher mortality risk in stroke patients (32) and other cerebral or cardiovascular diseases (summarized in *SI Appendix*, Table S2). This apparent discrepancy may reflect fundamental differences in Trem2 induction and its downstream inflammatory signaling between experimental stroke models and human disease. Indeed, our analysis of public transcriptomic datasets reveals that Trem2 is highly upregulated in stroke patients but not in mice subjected to MCAO. To address this limitation, we sought an experimental framework in which Trem2 is reliably induced after schemic stroke, reflecting a key clinical signature. Therefore, we employed the photothrombotic (PT) stroke model, which induces a well-demarcated cortical infarction accompanied by persistent, robust microglial activation and inflammatory responses (33, 34), aligning more closely with stroke patients (35). Using the PT model, we demonstrated significant Trem2 upregulation, and found that both Trem2 and sTrem2 confer exacerbate neuroinflammation, neuronal loss, and neurological deficits. These findings contrast with MCAO data but align with clinical observations. By integrating mouse and patient transcriptomic data, we identified glycoprotein nonmetastatic B (Gpnmb) as a key downstream Trem2-associated effector mediating lipid accumulation and microglial activation, highlighting the pathological role of Trem2 signaling and providing a potential therapeutic target in ischemic stroke.

Results

Trem2 Expression Is Increased in Stroke Patients. To investigate whether *Trem2* is upregulated in the human brain after stroke, we analyzed two independent transcriptomic datasets of brain tissues from stroke patients in the gene expression omnibus (GEO) database, encompassing both acute and chronic phases of the disease. In the first dataset (GSE162955), six brain samples were collected postmortem from ischemic stroke patients within 40 to 360 h of symptom onset, corresponding to the acute to subacute phase (36). Due to the small sample size, the authors of this dataset defined a q-value < 0.1 as significant. The *Trem2* mRNA level in the infarction core shows a strong trend toward increase compared to contralateral tissue (P = 0.0857) in this limited cohort, with four out of six patients showing increased *Trem2* expression in the infraction core (Fig. 1*A*). In the second dataset (GSE56267), ischemic cortical tissue from nonfatal stroke patients who later died of nonneurological causes was analyzed, typically 2 to 5 y after diagnosis, representing the chronic phase of stroke (37). We selected data from five nonstroke controls and five stroke patients matched for age and gender, as reported in the reference (38), to compare *Trem2* expression. *Trem2* expression in the infarcted cortex was nominally elevated, with 3.5 times higher than that in the cortical tissue from control individuals (P = 0.0543) (Fig. 1*B*).

To further investigate systemic *Trem2* expression, we examined peripheral blood transcriptomic datasets. In dataset GSE58294, which included 23 stroke patients and 23 control individuals, blood samples were obtained 24 h poststroke for microarray analysis (39). *Trem2* mRNA levels were significantly increased in stroke patients compared to controls (P = 0.0402) (*SI Appendix*, Fig. S1*A*). Consistently, analysis of dataset GSE22255 (40) revealed significantly increased *Trem2* expression in peripheral blood mononuclear cells (PBMCs) from 20 stroke patients 6 mo poststroke compared 20 matched healthy individuals (P = 0.0375) (*SI Appendix*, Fig. S1*B*). Overall, this evidence suggests that *Trem2* is increased during both the acute to subacute phase and the chronic phase of stroke, with persistent elevation in the ischemic brain and peripheral blood cells from stroke patients.

Trem2 Expression Is Not Upregulated in the MCAO Model. To examine *Trem2* expression in mouse MCAO paradigms, we analyzed published single cell RNA sequencing (scRNA-seq) datasets from the GEO database. Analysis of dataset GSE142445, which included ipsilateral and contralateral brain tissues collected at 4 h, 1 d, 3 d, or 7 d poststroke, along with three sham controls (41), revealed consistent cell and gene counts across samples (*SI Appendix*, Fig. S2*A*). The microglial population could be distinguished from other cell types, but its proportion did not increase in MCAO mice compared to the sham group (Fig. 1*C* and *SI Appendix*, Fig. S2*B*). *Trem2* expression was predominantly confined to the microglia population (*SI Appendix*, Fig. S2*C*). However, no significant change in *Trem2* levels was observed in the ipsilateral side compared to contralateral tissue at any examined time point after stroke or to uninjured sham animals (Fig. 1 *D* and *E*). Analysis of an independent MCAO scRNA-seq dataset (GSE225948) similarly showed that *Trem2* was predominantly expressed in the microglial cluster, but no significant upregulation was observed at 2 or 14 d after stroke (*SI Appendix*, Fig. S3 *A* and *B*). Also, there is detectable *Trem2* expression in peripheral blood cells from this MCAO dataset, albeit at lower levels than in microglia, with predominant expression in monocytes. No significant increase of *Trem2* expression was observed after stroke *SI Appendix*, Fig. S3 *C* and *D*).

We further validated the *Trem2* expression pattern in MCAO model using bulk RNA-seq datasets from the GEO database. Consistent with the scRNA-seq data, *Trem2* levels were not significantly increased in ischemic brain tissues or sorted microglia from the infarction region of the MCAO model (*SI Appendix*, Fig. S3*E*). In fact, *Trem2* expression was significantly decreased in sorted microglia from both mouse and rat MCAO models (*SI Appendix*, Fig. S3*E*).

Collectively, these findings suggest that *Trem2* expression is not consistently upregulated in the brain following MCAO-induced stroke.

Trem2 Expression Is Robustly Upregulated in the PT Model. The discrepancies between the outcomes of the MCAO animal model and stroke patients prompted us to investigate whether Trem2 can be reliably induced in an alternative ischemic model, namely the PT model. We extracted *Trem2* expression data from a published scRNA-seq dataset (42) and identified an approximately threefold upregulation of *Trem2* expression in the proximal peri-infarction area, while it was much less pronounced in the infarction core and distal peri-infarction area (*SI Appendix*, Fig. S3*F*). Based on these observations, we employed the PT model to quantify the upregulation of Trem2 on the mRNA and protein level (Fig. 1*F*). Compared with contralateral tissue, *Trem2* mRNA expression was elevated in both the infarction core and peri-infarction zone at 7 days post-injury (DPI) (Fig. 1*G*). Consistent with this, protein levels of Trem2 were also markedly increased in these regions,

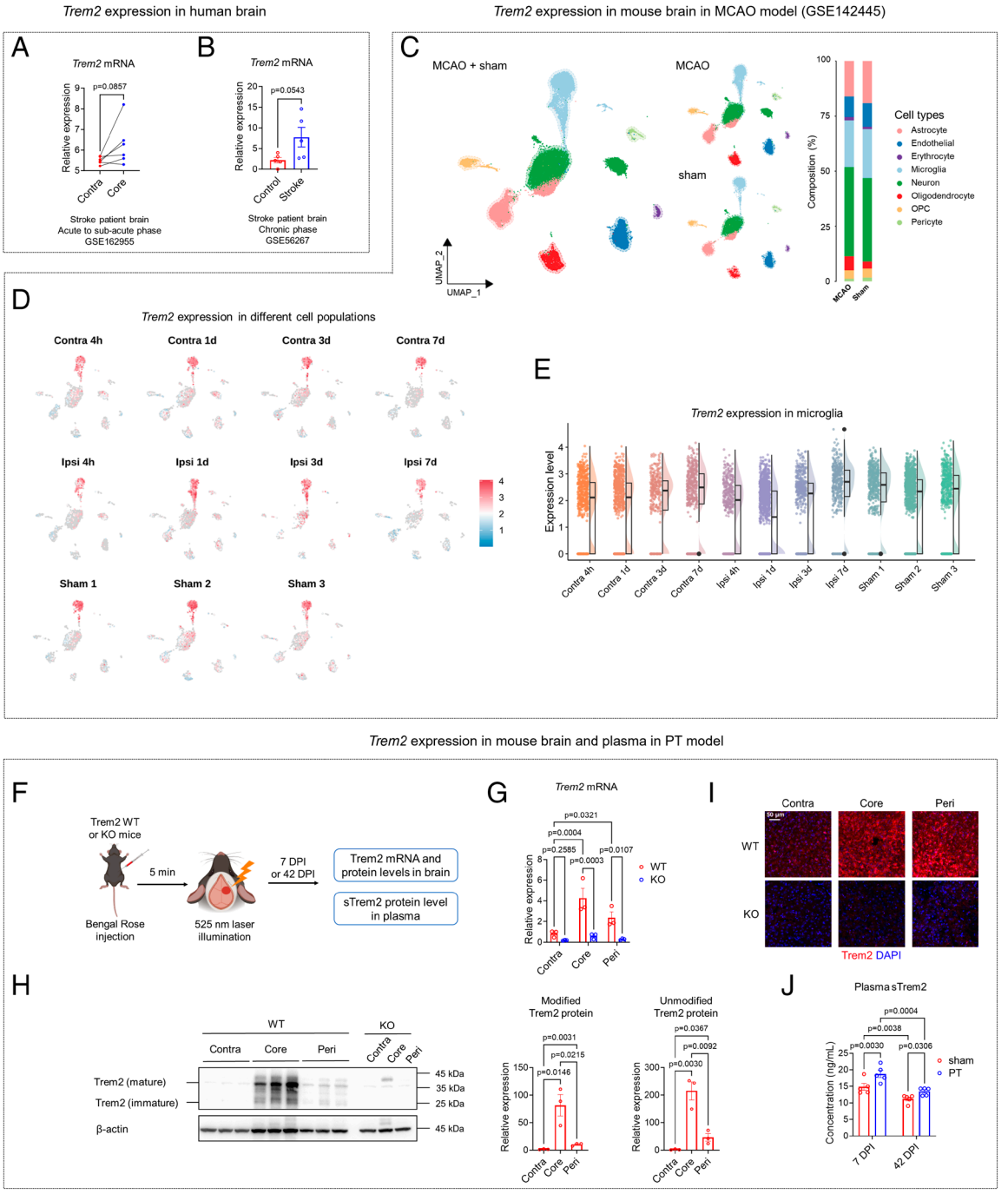

Fig. 1. Trem2 expression in stroke patients and animal models. (*A* and *B*) *Trem2* mRNA expression [–log2(counts + 1) normalized] in brains of stroke patients during the acute–subacute (n = 6) and chronic phases (n = 5), based on GEO datasets GSE162955 and GSE56267. (*C*–*E*) *Trem2* expression in a scRNA-seq dataset using mouse MCAO model (GSE142445). Uniform Manifold Approximation and Projection plots show cell classifications in MCAO and sham mice (*C*), with no increase in microglial proportion after MCAO. Trem2 is primarily expressed in microglia, with similar cell subpopulation distributions across sham, contralateral (Contra), or ipsilateral (Ipsi) samples at different time points (*D*), and no significant changes in microglial *Trem2* levels (*E*). (*F*) Experimental scheme of the photothrombotic (PT) stroke model. (*G*–*I*) *Trem2* mRNA (qPCR) (*G*), protein levels (western blot) (*H*), and immunostaining (*I*) at 7 days post-injury (DPI) in contralateral (Contra), infarction core (Core), and peri-infarction (Peri) regions (n = 3), normalized to wild-type (WT) contralateral controls. (*J*) Plasma sTrem2 levels in PT and sham mice at 7 and 42 DPI measured by the enzyme-linked immunosorbent assay (ELISA) (n = 5).

as shown by western blot (WB) analysis (Fig. 1*H*). Notably, a substantial portion of Trem2 protein shows molecular weight higher than the expected 25 kDa (Fig. 1*H*), consistent with posttranslational modification. Immunostaining further confirmed a robust increase in Trem2 expression in the injured region (Fig. 1*I*). Additionally, plasma sTrem2 levels were significantly elevated at both 7 DPI and 42 DPI in WT mice subjected to PT-induced stroke, compared to sham animals (Fig. 1*J*). As expected, in Trem2 KO animals, neither *Trem2* mRNA nor protein was changed at 7 DPI, as compared to WT animals (Fig. 1 *G*–*I*). Therefore, the PT model more accurately recapitulates this poststroke *Trem2* induction, presenting a translationally relevant system for dissecting the pathophysiological roles of Trem2 in ischemic stroke.

Trem2 Depletion Is Neuroprotective in PT-Induced Stroke. Next, we investigated whether the elevation of Trem2 in the PT model affects stroke parameters such as infarction volume or neurological

functions by comparing a Trem2-deficient mouse with a WT control (Fig. 2*A*). Limb motor impairment is a key symptom in ischemic stroke patients (43). To determine the impact of Trem2, we assessed the neurological and motor functions. At 7 DPI, Trem2 KO mice exhibited significantly better neurological performance compared to WT mice, as measured by the modified Neurological Severity Score (mNSS) (Fig. 2*B*), a widely used neurological test in rodents after stroke (34). In the foot fault test, Trem2 KO mice made significantly fewer missteps during 5 min locomotion at 1, 3, and 7 DPI compared to their WT littermates (*SI Appendix*, Fig. S4*A*). Similarly, in the rotarod test, Trem2-depleted mice showed less impaired motor coordination and endurance than WT animals (*SI Appendix*, Fig. S4*A*).

To analyze the neuroprotective effects of Trem2 depletion on a molecular and cellular level, brain tissue was collected at 7 DPI for histological and biochemical analyses (Fig. 2*A*). Extensive neuronal loss was observed in the cortical region at 7 DPI, as revealed by triphenyl tetrazolium chloride (TTC) staining and Nissl staining (*SI Appendix*, Fig. S4 *B* and *C*). The brain tissue was delineated into the infarction core, peri-infraction zone, and contralateral region using TTC staining, and the targeted regions were isolated for subsequent RNA or protein analysis (*SI Appendix*, Fig. S4*B*). Quantification of infarction volume, based on Nissl staining of cryosections, showed significantly smaller infarctions in Trem2 KO mice compared to WT animals (Fig. 2*C*).

In the infarction core, very few NeuN+ neurons were observed (*SI Appendix*, Fig. S4*C*). Consequently, subsequent analysis focused on NeuN+ cell density in the peri-infarction zone. While NeuN+ cell density was significantly decreased in both Trem2 WT and KO mice within this region compared to the contralateral side, neuronal loss was significantly less in Trem2 KO animals (Fig. 2*D*). To assess apoptosis, we performed cleaved caspase-3 positive (Cl.Casp3+) staining and terminal deoxynucleotidyl transferase dUTP nick end labeling (TUNEL) staining. Both the density of Cl.Casp3+ cells and their proportion relative to total DAPI+ cells were significantly higher in the peri-infarction zone

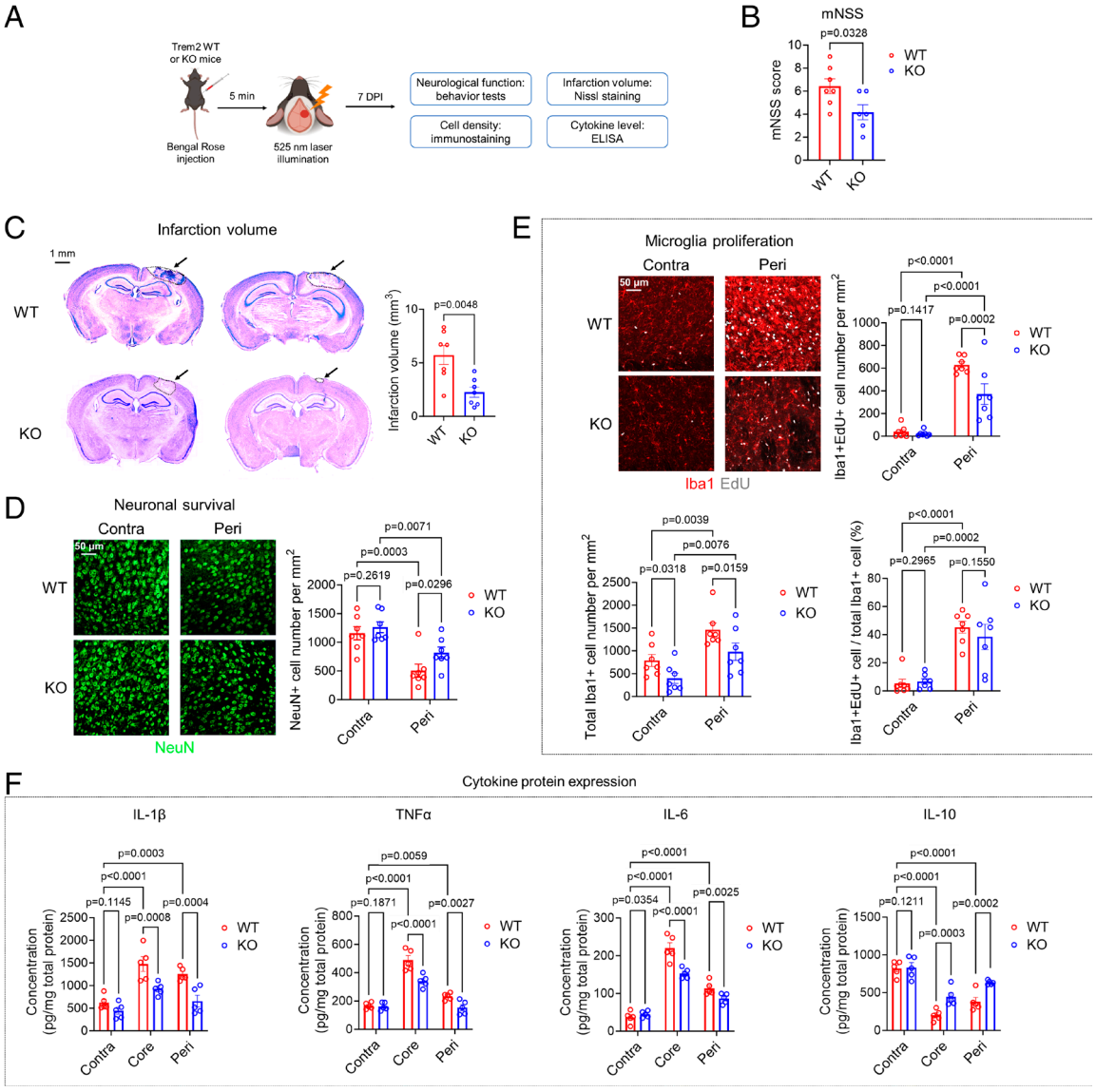

Fig. 2. Trem2 deficiency reduces ischemic injury and poststroke neuroinflammation. (*A*) Experimental scheme of PT-induced stroke in Trem2 WT and KO mice followed by assessments of neurological function, infarction size, neuronal survival, microglial proliferation, and cytokine expression. (*B*) Neurological function was evaluated by the mNSS at 7 DPI (WT: n = 7; KO: n = 6). (*C* and *D*) Nissl staining and NeuN immunostaining at 7 DPI were used to quantify infarction volume and peri-infarction neuronal survival in WT and KO mice (n = 7). (*E*) Iba1 and EdU costaining was performed to quantify total and proliferating microglia, as well as the proportion of proliferating microglia in the peri-infarction zone between genotypes (n = 7). (*F*) ELISA of IL-1β, TNFα, IL-6, and IL-10 levels in defined brain regions of WT and KO mice (n = 5).

compared to the contralateral side, yet this increase was significantly lower in Trem2 KO mice (*SI Appendix*, Fig. S4*D*). Similarly, the density and proportion of TUNEL+ late-stage apoptotic cells were remarkably elevated in the infarction core, while Trem2 depletion resulted in a significantly lower apoptotic cell density (*SI Appendix*, Fig. S4*E*). Since neural stem/progenitor cells (NSPCs) are known to migrate from the subventricular zone to the injured area after stroke (44), we examined both the density of proliferating NSPCs and their proportion relative to total Sox2+ NSPCs in the peri-infarction zone. Proliferating NSPCs were identified by colabeling Sox2 with the proliferation marker ethidium bromide (EdU). In the uninjured region, very few proliferating NSPCs were detected. Although the density and the proportion of these proliferating cells was higher in the peri-infarction zone, no difference was observed between Trem2 WT and KO mice (*SI Appendix*, Fig. S4*F*). This finding suggests that the reduced neuronal loss in Trem2 KO mice is not attributable to enhanced neurogenesis. In addition, we investigated whether the blood vessel area was influenced by Trem2 depletion after stroke. The area of CD31+ labeling, indicative of vascular endothelial cells, was larger in the peri-infarction zone compared to contralateral tissue. However, no difference was observed between Trem2 WT and KO groups (*SI Appendix*, Fig. S4*G*), suggesting that Trem2 does not affect blood vessel area in the peri-infarction zone after stroke. In summary, our results indicate that Trem2 depletion confers neuroprotection, reduces infarction volume, and enhances neurological functions following ischemic stroke, independent of neurogenesis and blood vessel area.

Trem2 Depletion Results in Lower Microglial Density. In the peri-infarction zone, Iba1+ microglia and GFAP+ astrocytes proliferated and accumulated in both Trem2 WT and KO mice (*SI Appendix*, Fig. S5*A*). Proliferating microglial cells were identified by colabeling with EdU and the microglial marker Iba1 (*SI Appendix*, Fig. S5*B*). As expected, the density of both total and proliferating microglia significantly increased in the injury regions relative to contralateral tissue. However, the density of both total and proliferating microglia was significantly lower in Trem2 KO animals, while the proportion of proliferating microglia relative to the total microglia remained unchanged between the two genotypes (Fig. 2*E*). Furthermore, the expression of CD68, a glycoprotein indicating lysosomal activity associated with phagocytosis, was significantly elevated as revealed by an increase of the CD68+ fluorescence area in the peri-infarction zone of WT mice, whereas the CD68+ area was significantly lower in KO animals (*SI Appendix*, Fig. S5*C*). Similarly, the density of both total (GFAP+) and proliferating (GFAP+EdU+) astrocytes was also remarkably increased in the peri-infarction zone of WT controls, but this increase was lower in Trem2-depleted animals (*SI Appendix*, Fig. S5 *A* and *D*), mirroring the pattern observed in microglia. The proportion of proliferating astrocytes relative to the total astrocytes remained consistent across genotypes (*SI Appendix*, Fig. S5*D*). Taken together, our data suggest that Trem2 is required for the proliferative response of microglia and astrocytes following stroke, and its absence attenuates the expansion of these glial populations after injury.

Additionally, we utilized the distal middle cerebral artery occlusion (dMCAO) model, a permanent MCA occlusion model (45), to compare Trem2 expression and its associated phenotypic effects with those observed in the PT model (*SI Appendix*, Fig. S6*A*). Using appropriate sham controls for both PT and dMCAO, we confirmed that sham procedures did not affect neurological function, induce infarction, or trigger Trem2 expression (*SI Appendix*, Fig. S6 *B*–*D*). Although the dMCAO model produced neurological deficits comparable to those in the PT model (*SI Appendix*, Fig. S6*B*) and even resulted in larger infarction volumes (*SI Appendix*, Fig. S6*C*), the increase in Trem2+Iba1+ cell coverage at 7 DPI was not significant compared to the dMCAO sham group, but significantly lower than that observed in the PT model (*SI Appendix*, Fig. S6*D*). Collectively, these results suggest that the PT model may be more suitable than dMCAO for studying Trem2 function.

Trem2 Depletion Attenuates Stroke-Induced Cytokine Expression. Cytokines are key mediators of neuroinflammation and orchestrate the immune response to ischemic injury (46). To investigate whether the absence of Trem2 alters cytokine expression, we isolated tissues from the infarction core, peri-infarction zone, and contralateral region following TTC staining at 7 DPI. The protein levels of pro- and anti-inflammatory cytokines were measured using ELISA. IL-1β and TNFα, two principal proinflammatory cytokines, were significantly elevated in the infarction core and peri-infarction zone compared to the contralateral region. However, this elevation was significantly blunted in Trem2 KO mice (Fig. 2*F*). Similarly, IL-6, a pleiotropic cytokine with both pro- and anti-inflammatory properties, was elevated in both the infarction core and peri-infarction zone. Notably, the increase of IL-6 was attenuated by Trem2 depletion (Fig. 2*F*). In contrast, anti-inflammatory IL-10 was notably suppressed in the ischemic regions of WT animals, while Trem2 deficiency ameliorated this suppression (Fig. 2*F*). These observations were corroborated using an in vitro microglia model mimicking an ischemic insult. Cells from the microglial cell line BV2 were subjected to oxygen-glucose deprivation (OGD), a standard in vitro model of ischemia (*SI Appendix*, Fig. S7*A*). *Trem2* expression was silenced using two different lentivirus-packaged shRNAs. *Trem2* mRNA expression was effectively downregulated with targeted shRNAs. While *Trem2* mRNA levels were significantly increased following OGD treatment in control cells, this increase was abolished in the *Trem2*-knockdown cells (*SI Appendix*, Fig. S7*B*). Similarly, protein levels of Trem2 were elevated in control cells after OGD but were nearly undetectable in *Trem2*-knockdown cells, both in cell lysates and as secreted sTrem2 in culture medium (*SI Appendix*, Fig. S7*C*). The mRNA levels of *Tnf*, *Il-1b*, and *Il-6* were significantly upregulated after OGD treatment, and this increase was attenuated in *Trem2*-silenced cells (*SI Appendix*, Fig. S7*D*). However, the expression of *Il-10* was not significantly influenced by Trem2 downregulation (*SI Appendix*, Fig. S7*D*). The in vitro results in BV2 cells align with the in vivo findings, supporting the hypothesis that Trem2 regulates microglial cytokine responses to ischemic injury. These data suggest that Trem2 deficiency suppresses the proinflammatory cytokine expression.

sTrem2 Exacerbates Ischemic Injury by Amplifying Neuroinflammation. Recent clinical studies have identified sTrem2 as a potential risk factor for ischemic stroke and related vascular diseases (*SI Appendix*, Table S2). Based on these findings, we hypothesized that sTrem2 may exacerbate ischemic injury. To test this hypothesis, recombinant sTrem2 protein or phosphate-buffered saline (PBS) control was injected into the targeted injury region 1 h prior to PT treatment (Fig. 3*A*). After injection, recombinant sTrem2 diffused throughout the targeted injury region, persisting up to 6 h, with substantial reduction observed at 24 h postinjection (*SI Appendix*, Fig. S5*E*). At 7 DPI, sTrem2-treated WT animals exhibited significantly worse neurological function, as assessed by the mNSS, compared to PBS-treated controls (Fig. 3*B*). Histological analysis revealed markedly larger infarction volumes in the sTrem2-treated group compared to the PBS-treated controls (Fig. 3*C*). Concomitantly, neuronal density was significantly reduced in the peri-infarction zone of sTrem2-treated mice (Fig. 3*D*). Furthermore, the density of both total

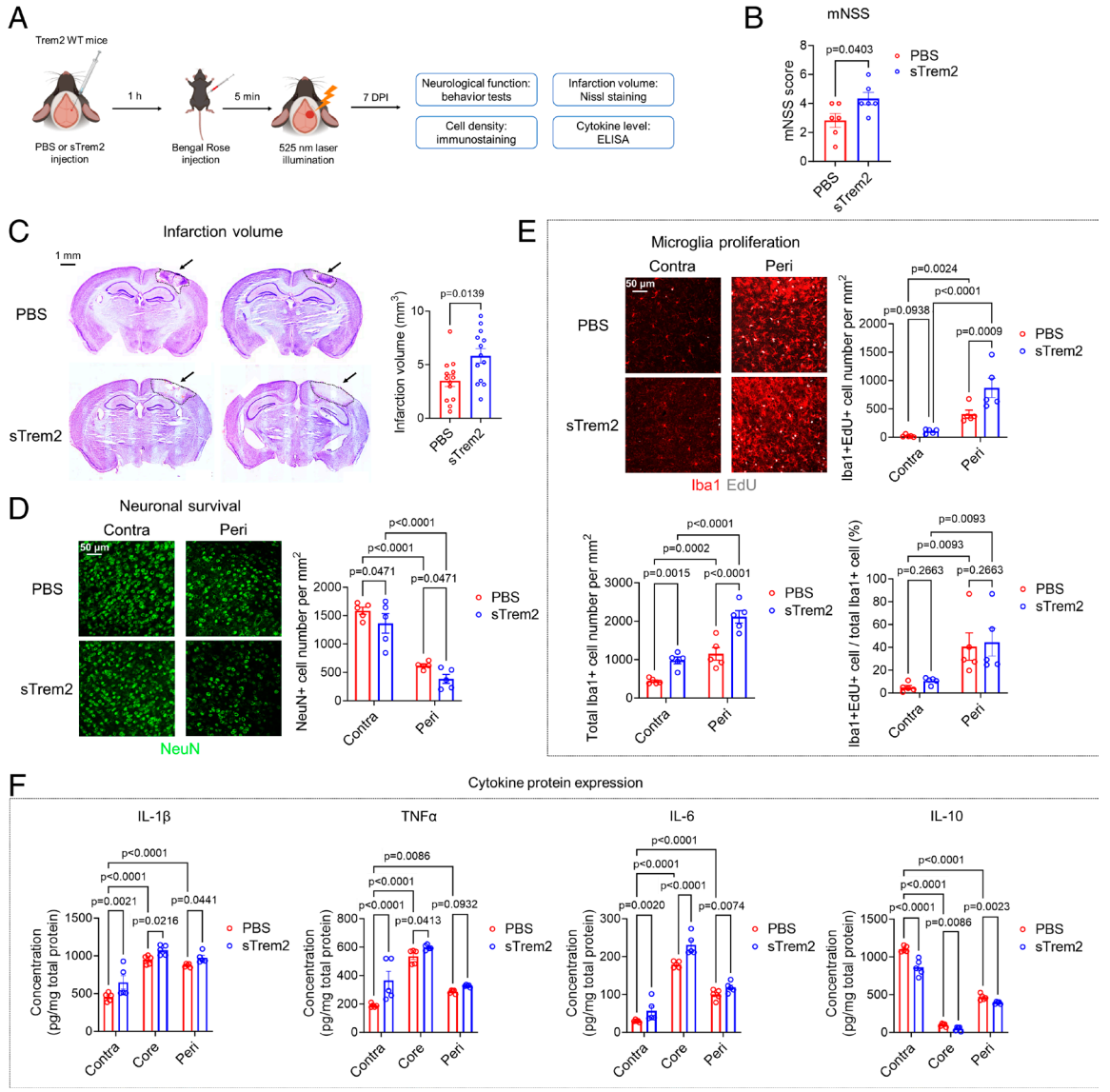

Fig. 3. sTrem2 aggravates ischemic injury and poststroke neuroinflammation. (*A*) Experimental scheme of recombinant sTrem2 or PBS injection before PT-induced stroke, followed by assessments of neurological function, infarction size, neuronal survival, microglial proliferation, and cytokine expression. (*B*) Neurological function was evaluated by mNSS at 7 DPI in sTrem2- and PBS-treated mice (n = 6). (*C* and *D*) Nissl staining and NeuN immunostaining at 7 DPI were used to quantify infarction volume and peri-infarction neuronal survival in the two groups (*C*: n = 13; *D*: n = 5). (*E*) Iba1 and EdU costaining was performed to quantify total and proliferating microglia, as well as the proportion of proliferating microglia in the peri-infarction zone between groups (n = 5). (*F*) ELISA of IL-1β, TNFα, IL-6, and IL-10 levels in defined brain regions (n = 5).

and proliferating microglia was substantially increased in the peri-infarction zone of sTrem2-treated mice compared to PBS control, although the proportion of proliferating microglia relative to the total microglial population remained unchanged (Fig. 3*E*). In parallel, the cytokine levels of IL-1β, TNFα, and IL-6 were significantly elevated in the infarction core, peri-infarction zone, and even the contralateral side of the sTrem2-injected group (Fig. 3*F*). In contrast, IL-10 levels in these regions were decreased in the sTrem2-injected group (Fig. 3*F*). These findings suggest that sTrem2 further stimulates microglia activation, promotes neuroinflammation, and exacerbates neuronal damage in PT-induced ischemic model.

Trem2 Depletion Alters Transcriptomic Patterns and Microglia Subpopulations After Stroke. To elucidate the molecular mechanisms by which Trem2 affects the outcome in stroke, we performed bulk RNA-seq on brain tissues isolated from the infarction core, peri-infarction zone, and contralateral region of Trem2 WT and KO mice at 7 DPI. Gene expression analysis revealed approximately 2,000 to 8,000 differentially expressed genes (DEGs), both up- and downregulated, when comparing the infarction core or peri-infarction zone to the contralateral tissue, regardless of genotype (KO or WT). However, genotype-specific comparisons (KO vs. WT) identified only 341 DEGs in the peri-infarction zone, with even fewer DEGs detected in the infarction core and contralateral tissue (*SI Appendix*, Fig. S8*A*). Heatmap analysis demonstrated Trem2-dependent alterations in gene expression across these different regions (*SI Appendix*, Fig. S8*B*). These findings indicate that Trem2 depletion drives substantial transcriptional alterations in the peri-infarction zone, while the infarction core and contralateral tissue are less affected. Gene ontology analysis of DEGs from all three regions demonstrated enrichment in immune-related processes, suggesting Trem2 modulates microglia-mediated inflammatory responses (*SI Appendix*, Fig. S8 *C–E*). Kyoto Encyclopedia of Genes and Genomes analysis revealed that, although genes involved in

various immune responses were enriched across all three regions, only the peri-infarction zone exhibited signaling pathways with reliable q values. These pathways included the complement and coagulation cascade, as well as phagosomal and lysosomal functions (*SI Appendix*, Fig. S8*F*). This finding aligns with higher DEG count in the peri-infarction zone.

Given that Trem2 expression is a hallmark of disease-associated microglia (DAM) under pathological conditions (47), we performed cellular deconvolution analysis to evaluate the impact of Trem2 depletion on DAM populations during PT-induced stroke. While disease-associated glial cell subtypes are well characterized in AD models, they remain less defined in stroke models. To address this, we used marker genes from the published scRNA-seq dataset GSE243018 from AD model to cluster DAMs, following an approach similar to previous study (48). We also analyzed the scRNA-seq dataset GSE142445 from a stroke model to classify general brain cell types. Based on established criteria (49), we defined microglia subpopulations as homeostatic microglia, interferon-responsive microglia (IRM), DAM, and major histocompatibility complex class II (MHC class II)-expressing microglia (MHC-II), each characterized by distinct cellular markers (Fig. 4*A* and *SI Appendix*, Fig. S9 *A* and *B*). Among these, the DAM2 subpopulation exhibited rapid expansion following stroke, accompanied by increases in DAM1 and MHC-II microglia as well (*SI Appendix*, Fig. S9*C*). To further explore these dynamics, we integrated our bulk RNA-seq data for cellular deconvolution analysis. As expected, there was a pronounced increase in the proportion of microglia within the infarction core and peri-infarction zone. In agreement with our histological data, microglia proportion was significantly decreased in Trem2 KO mice (*SI Appendix*, Fig. S9*D*). Further analysis of microglial subpopulations revealed a substantial shift in response to Trem2 depletion, which was associated with a marked reshaping of poststroke microglial states. The increase in IRM microglia, which typically expands during the acute stage of neurological disease (50), together with elevated DAM1 microglia in Trem2 KO mice suggests that Trem2 depletion disrupts the progression of microglia toward more activated inflammatory programs, including DAM2 and MHC-II–associated states (49) (Fig. 4*B*), thereby reshaping the neuroinflammatory landscape following ischemic stroke.

Gpnmb Is a Trem2-Dependent Factor Conserved Across Mouse and Human Stroke Patients. To assess the clinical relevance of these DEGs identified in Trem2 WT and KO mice, we analyzed these DEGs in the human GSE162955 dataset (36), which includes brain samples from the ipsilateral and contralateral

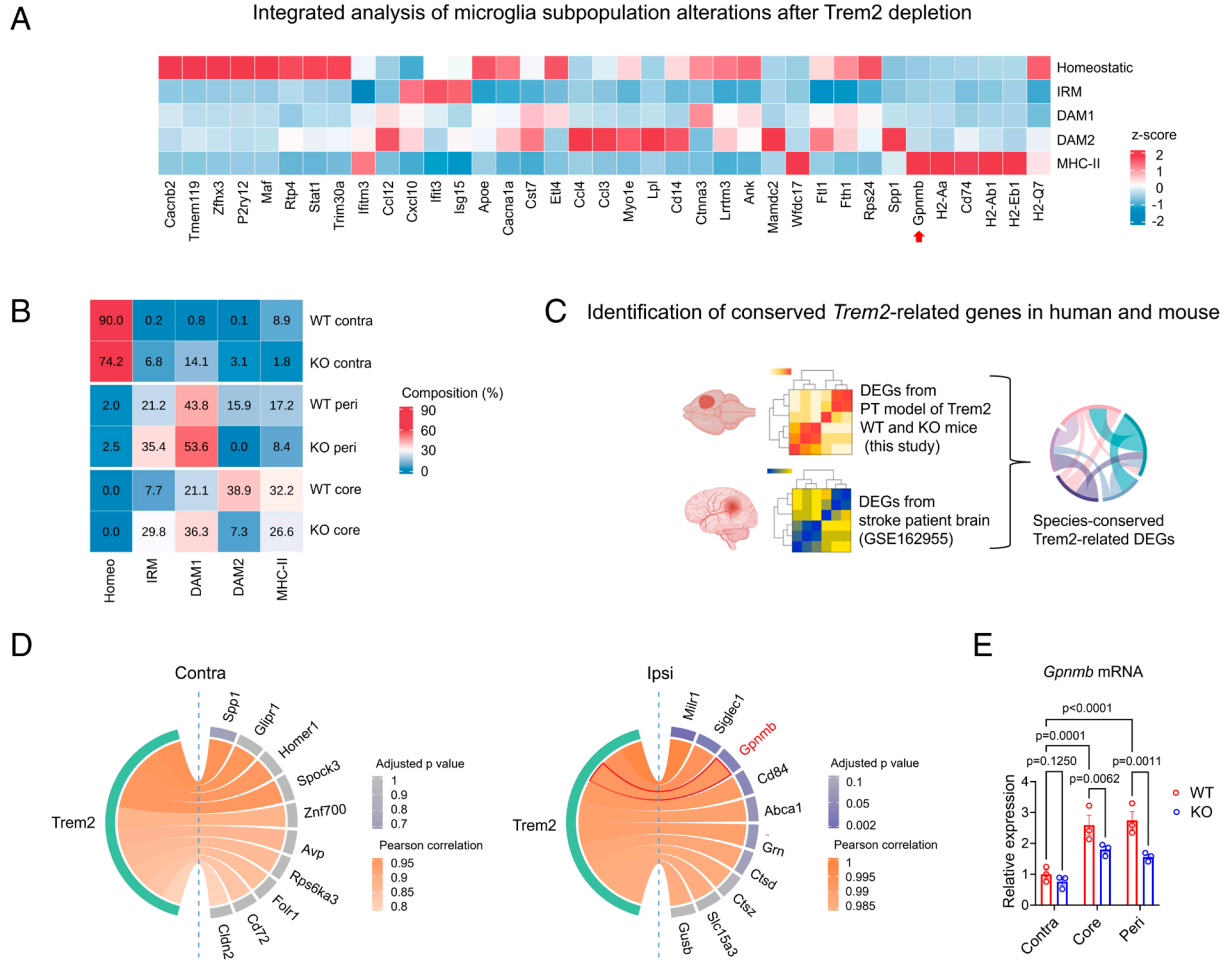

Fig. 4. Integrated transcriptomic analysis reveals Gpnmb as a downstream effector of Trem2 after ischemic stroke. (*A* and *B*) Deconvolution analysis of microglial subpopulations in PT-induced stroke. Heatmaps show marker gene expression used to define microglial subsets (homeostatic, IRM, DAM1, DAM2, MHC-II) in GSE243018 dataset (*A*). Deconvolution analysis was performed to estimate subpopulation proportions in Trem2 WT and KO mice using GSE142445 dataset as reference. PT-induced stroke reduces homeostatic microglia and increases IRM, DAM1, DAM2, and MHC-II subsets, whereas DAM2 and MHC-II populations in peri-infarction zone and infarction core are reduced in Trem2 KO mice (*B*). (*C* and *D*) Integrated mouse-human transcriptomic analysis (*C*) identifies conserved *Trem2*-associated genes. Four genes (*Milr1*, *Siglec1*, *Gpnmb*, *Cd84*) show strong correlation with *Trem2* in ipsilateral tissue (R > 0.99, adjusted $P < 0.05$) (*D*). (*E*) *Gpnmb* mRNA expression in PT mouse brains at 7 DPI was measured by qPCR and normalized to WT contralateral tissue (n = 3).

regions of stroke tissue from patients in the acute to subacute phase. This allowed us to evaluate the correlation between *Trem2* expression and DEGs (Fig. 4*C*). Correlation analysis of DEGs from the contralateral region revealed no significant associations with *Trem2*. However, when we evaluated the DEGs from peri-infraction zone and infraction core (Trem2 WT vs. KO) and asked whether these genes correlated with *Trem2* expression levels in the human dataset from ipsilateral stroke tissue, four genes (*Milr1*, *Siglec1*, *Gpnmb*, and *Cd84*) demonstrated strong positive correlations with *Trem2* expression ($R > 0.99$ and adjusted $P < 0.05$). *Abca1* demonstrated a near-significant correlation ($R = 0.9898$ and adjusted $P = 0.0599$) (Fig. 4*D*). These genes appeared to be conserved in their alteration following stroke in both mice and humans. However, *Milr1*, *Siglec1*, *Cd84*, and *Abca1* could not be successfully validated by qPCR in our mouse model (*SI Appendix*, Fig. S9*E*). Instead, qPCR results confirmed that *Gpnmb* (glycoprotein nonmetastatic melanoma protein B) expression was significantly upregulated in the peri-infarction zone and infarction core of WT mice. This induction was markedly diminished in Trem2 KO animals, suggesting that *Gpnmb* upregulation is Trem2-dependent (Fig. 4*E*).

In recent years, *Gpnmb* has been reported to positively correlate with *Trem2* expression in various pathological conditions, including AD, glioblastoma, and atherosclerosis (51–53). To further explore this relationship, we analyzed our RNA-seq data from Trem2 KO and WT mice in the PT stroke model using inflammation-related gene set enrichment analysis (GSEA). The results revealed that both *Trem2* and *Gpnmb* are positively associated with tumor necrosis factor (TNF) superfamily cytokine production and leukocyte proliferation (*SI Appendix*, Fig. S10*A*). In transcriptomic datasets of stroke patient brains (GSE162955), *Gpnmb* showed a strong positive correlation with *Trem2* in the acute-to-subacute phase in the ipsilateral region, but not in the contralateral region (*SI Appendix*, Fig. S10*B*). Interestingly, although *Gpnmb* expression was not significantly induced during this phase, its expression was markedly elevated in the chronic phase (GSE56267) (*SI Appendix*, Fig. S10 *B* and *C*). Furthermore, a positive correlation with *Trem2* was observed in both the chronic-phase stroke and control groups (*SI Appendix*, Fig. S10*C*). Additionally, we analyzed the published scRNA-seq datasets from PT models (42) to further validate this correlation. In the PT stroke model, *Gpnmb* expression was significantly upregulated in the proximal peri-infarction area, but was much less prominent in the infarction core and distal peri-infarction area (*SI Appendix*, Fig. S10*D*), mirroring the expression pattern of *Trem2* (*SI Appendix*, Fig. S3*F*). However, in the MCAO stroke model, where Trem2 is not upregulated, *Gpnmb* expression was relatively low and not enriched in microglia (*SI Appendix*, Fig. S10*E*), strengthening our hypothesis that Gpnmb expression is regulated by Trem2. Notably, among microglial subpopulations after stroke, MHC-II microglia appears to be the only subpopulation expressing *Gpnmb* (Fig. 4*A*), suggesting that Trem2-mediated effects may preferentially target this specific microglial subpopulation.

To confirm the association between Trem2 and Gpnmb at the protein level, we performed WB and immunohistochemistry on brain tissue from PT stroke mice. WB analysis detected Gpnmb as double bands (~100 kDa) rather than the expected 70 kDa (*SI Appendix*, Fig. S11*A*), likely reflecting posttranslational modifications such as glycosylation and phosphorylation, as previously reported (54). Consistent with the qPCR results (Fig. 4*E*), Gpnmb protein levels were significantly elevated in both the peri-infarction zone and infarction core, with this elevation markedly attenuated in Trem2-depleted animals (*SI Appendix*, Fig. S11*A*). Immunostaining revealed that Gpnmb localized predominantly to Iba1+ microglia within the peri-infarction zone, with reduced expression observed in Trem2 KO mice (*SI Appendix*, Fig. S11 *B* and *C*). Notably, Gpnmb expression levels in the peri-infarction zone were further enhanced in sTrem2-treated WT mice compared to PBS-treated control animals following PT-induced stroke (*SI Appendix*, Fig. S11*D*). Since Gpnmb is implicated in lipid metabolism (55), we measured lipid droplet accumulation by quantifying BODIPY+ cells in the peri-infarction zone. Similar to Gpnmb expression, BODIPY coverage was decreased in KO mice but significantly increased in sTrem2-treated animals (*SI Appendix*, Fig. S11 *C* and *D*). Collectively, our data highlight Gpnmb as a Trem2-dependent factor conserved across mouse models and human stroke patients, suggesting that Gpnmb may represent a critical downstream effector of Trem2 in ischemic stroke.

Soluble Gpnmb (sGpnmb) Diminishes the Protective Effect of Trem2 Depletion After Stroke. To determine whether Gpnmb functions downstream of Trem2 and mediates the Trem2-induced neurotoxic effects, we used BV2 cells subjected to the OGD model (*SI Appendix*, Fig. S12*A*). Similar to the in vivo results, both mRNA and protein levels of Gpnmb were elevated following OGD treatment. As expected, *Gpnmb* mRNA expression and protein levels were significantly reduced in *Trem2*-silenced BV2 cells after OGD (*SI Appendix*, Fig. S12 *B* and *C*), confirming that Gpnmb is positively regulated by Trem2. Additionally, the soluble form of Gpnmb (sGpnmb) in the culture medium was similarly upregulated following OGD but was markedly decreased in *Trem2*-silenced BV2 cells (*SI Appendix*, Fig. S12*C*). To investigate the functional implications of these microglial changes on neuronal survival, conditioned medium from BV2 cells was applied to the mouse hippocampal neuronal cell line HT-22, followed by thiazolyl blue tetrazolium bromide viability assays (*SI Appendix*, Fig. S12*A*). The viability of HT22 cells was unaffected by conditioned medium from control or *Trem2*-silenced BV2 cells under normal culture conditions (*SI Appendix*, Fig. S12*D*). In contrast, conditioned medium from OGD-treated BV2 cells caused significant cytotoxicity, which was mitigated by *Trem2* knockdown (*SI Appendix*, Fig. S12*D*). Interestingly, supplementation with recombinant sTrem2 or sGpnmb in the BV2-conditioned medium increased its cytotoxicity to HT-22 cells, regardless of either the conditioned medium was from control or OGD-treated BV2 cells (*SI Appendix*, Fig. S12*D*). Furthermore, adding sGpnmb diminished the neuroprotective effects of *Trem2* knockdown (*SI Appendix*, Fig. S12*D*). In addition, we examined whether Trem2 directly modulates microglial responses to OGD or neuronal cell debris (*SI Appendix*, Fig. S12*E*). BV2 cells were activated upon exposure to debris from HT-22 cells subjected to OGD, and their conditioned medium subsequently reduced the viability of a new batch of HT-22 cells. However, *Trem2* knockdown did not alter the microglial response to neuronal debris, as the effects on HT-22 cell viability remained unchanged (*SI Appendix*, Fig. S12*F*). We also quantified BODIPY+ lipid droplets in BV2 cells with or without OGD treatment. In the absence of OGD, minimal BODIPY+ lipid signals were observed. OGD treatment induced a substantial increase in BODIPY+ lipid droplets, which was attenuated by *Trem2* downregulation. However, this attenuation was reversed by the addition of recombinant sGpnmb (*SI Appendix*, Fig. S12*G*).

In the animal PT model, we injected recombinant sGpnmb protein or PBS into the targeted injury region of Trem2 WT or KO mice 1 h before PT treatment (Fig. 5*A*), following a protocol similar to the previous experiment with sTrem2 injection. In PBS-treated animals, we again detected a protective effect of Trem2 deletion with reduced mNSS scores as compared to WT animals; however, this protection

was abrogated by sGpnmb pre-injection (Fig. 5*B*). sGpnmb pre-injection nullified Trem2-deficiency-induced alterations in infarction volume, neuronal survival, and microglial proliferation within the peri-infarction zone. Infarction volumes in sGpnmb-treated KO animals were significantly larger than in PBS-treated KO animals (Fig. 5*C*). Consistently, neuronal numbers were significantly reduced in the peri-infarction zone of Trem2 KO mice treated with sGpnmb compared to PBS treatment (Fig. 5*D*). In parallel, the density of both total and proliferating microglia was increased in sGpnmb-treated Trem2 KO mice relative to PBS-treated counterparts; however, the proportion of proliferating microglia relative to the total microglial population remained unchanged (Fig. 5*E*). Furthermore, Gpnmb and BODIPY signals were almost absent at the contralateral side (*SI Appendix*, Fig. S13*A*) but were significantly elevated in the peri-infarction zone of the sGpnmb-treated group compared to the PBS-treated group in Trem2 KO mice (Fig. 5*F*). To further elucidate the role of Trem2 in lipid metabolism, we performed lipid metabolism-related GSEA using our RNA-seq data from Trem2 WT and KO mice following PT-induced stroke, similar to *SI Appendix*, Fig. S10*A*. The analysis confirmed that Trem2 is positively associated with lipid homeostasis, lipid localization and its positive regulation, and lipid storage (*SI Appendix*, Fig. S13*B*). Collectively, our findings suggest that Gpnmb/sGpnmb is a downstream effector of Trem2, promoting lipid droplet accumulation in microglia and ultimately exacerbating neuronal death in ischemic stroke.

Plasma Trem2 and Gpnmb Levels Are Associated with Unfavorable Stroke Outcomes. Next, we examined the protein levels of sTrem2 and sGpnmb in the plasma samples from stroke patients and controls. The clinical characteristics of the enrolled stroke patients and control individuals are summarized in *SI Appendix*, Table S3. Whole blood samples were collected approximately 24 h after symptom onset, and plasma was isolated for subsequent analysis (Fig. 6*A*). Plasma protein levels of both sTrem2 and sGpnmb were significantly elevated in stroke patients compared to controls (Fig. 6*B*). Notably, strong correlations between plasma sTrem2 and sGpnmb were observed in plasma from both control individuals and stroke patients (Fig. 6*C*). To assess the potential of plasma sTrem2 and sGpnmb as biomarkers of stroke severity, we evaluated neurological functions using the National Institute of Health Stroke Scale (NIHSS), Fugl-Meyer Assessment (FMA), Modified Barthel Index (MBI), and Stroke Scales of Traditional Chinese Medicine (SSTCM). The 16 patients were stratified into two groups based on their performance in these assessments. The group with favorable outcomes demonstrated significantly lower NIHSS and SSTCM scores and higher FMA and MBI scores, compared to the group with poor outcomes (*SI Appendix*, Fig. S14). Plasma sTrem2 levels were significantly higher in the group with poor outcomes (Fig. 6*D*). Plasma sGpnmb levels tended to be higher in the poor-outcome group, although the difference did not reach statistical significance, which is likely attributable to the small sample size of this subgroup (Fig. 6*D*). Receiver-operating characteristic (ROC) curve analysis further demonstrated that plasma levels of both sTrem2 and sGpnmb accurately predicted stroke severity, with high sensitivity and specificity (Fig. 6*E*). These results indicate that elevated plasma sTrem2 and sGpnmb levels are associated with unfavorable neurological outcomes following stroke, highlighting their potential as circulating biomarkers.

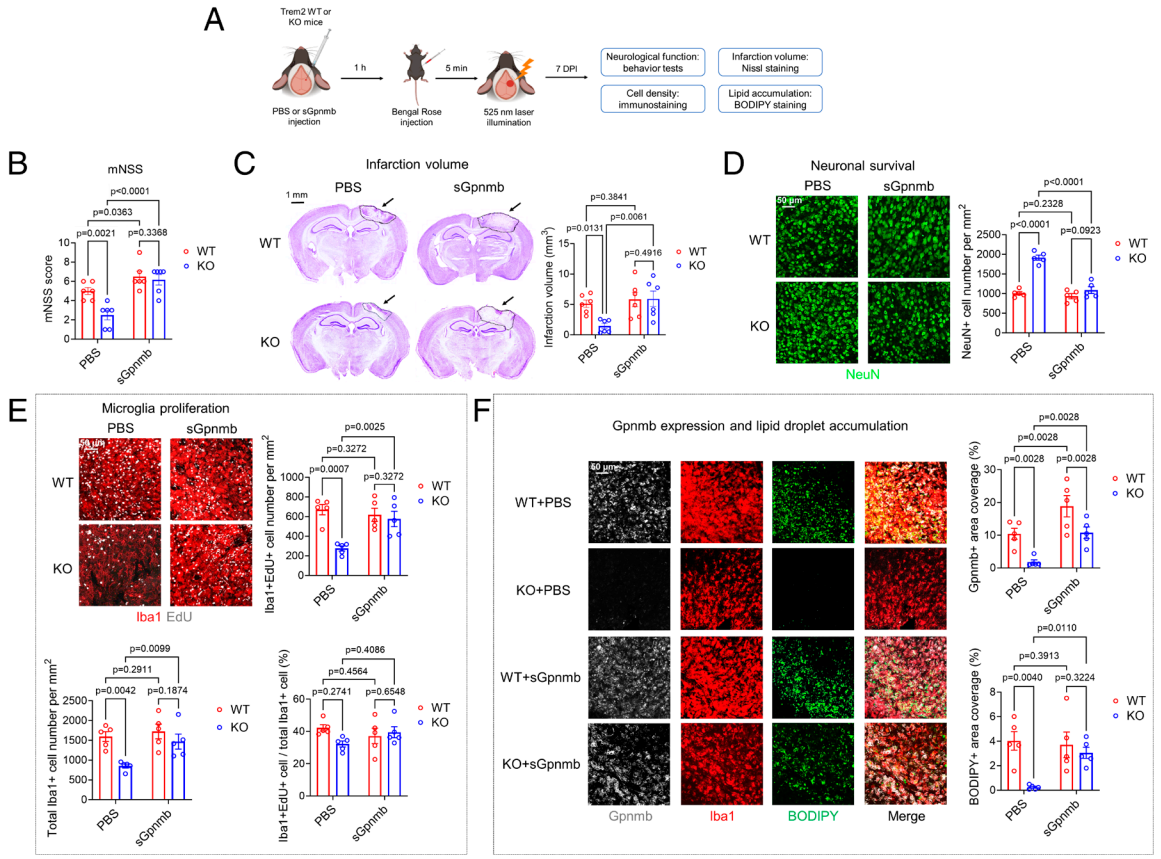

Fig. 5. sGpnmb reverses the protective effects of Trem2 deficiency after PT-induced stroke. (*A*) Scheme of intracerebral recombinant sGpnmb or PBS injection into Trem2 WT or KO mice before PT stroke. (*B*) Neurological function assessed by mNSS at 7 DPI (n = 6). (*C* and *D*) Nissl staining (*C*) and NeuN immunostaining (*D*) at 7 DPI quantified infarction volume and peri-infarction neuronal survival across groups (*C*: n = 6; *D*: n = 5). (*E*) Iba1 and EdU costaining quantified total and proliferating microglia, and their proportion, in the peri-infarction zone (n = 5). (*F*) Gpnmb, Iba1, and BODIPY immunostaining assessed Gpnmb expression and lipid droplet accumulation in the peri-infarction zone (n = 5).

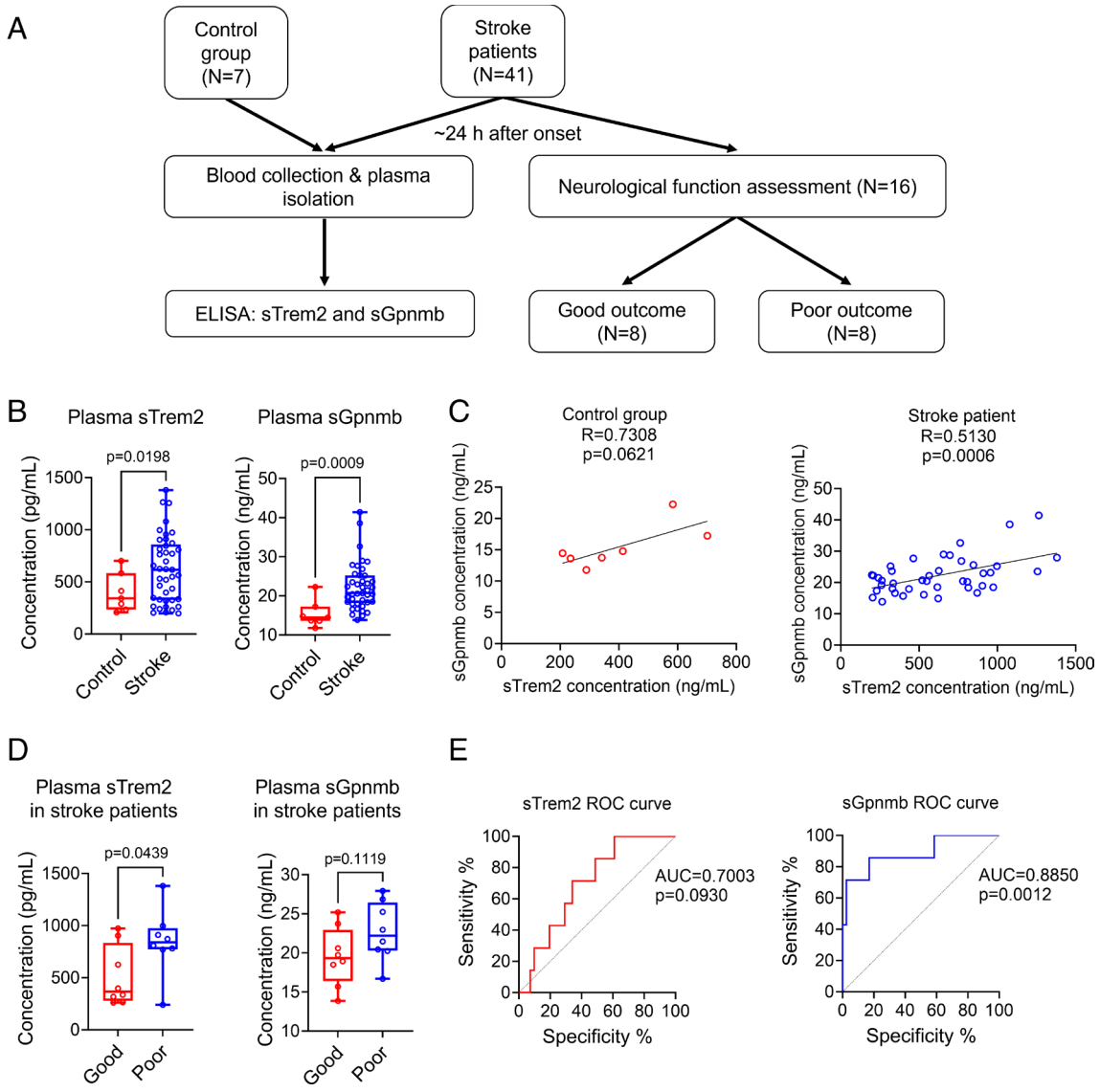

Fig. 6. Plasma sTrem2 and sGpnmb correlate with poor stroke outcomes in patients. (*A*) Clinical study design: Blood was collected from patients and controls for plasma sTrem2 and sGpnmb measurement by ELISA; neurological function was assessed. (*B*) Plasma sTrem2 and sGpnmb levels in controls (n = 7) and stroke patients (n = 41). (*C*) Correlation between plasma sTrem2 and sGpnmb. (*D*) Levels of sTrem2 and sGpnmb in patients with good vs. poor outcomes (n = 8). (*E*) ROC curves show predictive value of sTrem2 and sGpnmb for stroke outcomes.

Discussion

Neuroinflammation plays dual roles in brain injury and neurodegeneration, with microglia promoting neuronal survival or contributing to secondary damage in a disease- and stage-specific manner (56, 57). Trem2 is a key modulator of microglial function, balancing protective and detrimental effects (58). While Trem2 is generally considered protective in AD (59, 60), its role in ischemic stroke remains controversial. Our study shows that Trem2 is upregulated in the PT model but not in distal or transient MCAO, suggesting PT is more appropriate for studying Trem2 in stroke. Trem2 depletion reduces infarction volume, neuronal loss, and neuroinflammation, accompanied by decreased Gpnmb expression and lipid droplet accumulation in microglia, highlighting Gpnmb as a downstream effector. sGpnmb counteracts these benefits and elevated plasma sTrem2 and sGpnmb correlate with poor outcomes in stroke patients, underscoring their potential as biomarkers. These findings are summarized in *SI Appendix*, Fig. S15. A key limitation of this study is that the animal experiments were conducted exclusively in young male mice housed under specific-pathogen-free (SPF) conditions, which may influence innate immune responses. Future studies should examine the potential effects of age and sex as variables that may modulate Trem2 function, and consider the use of wild or non-SPF mice with more ecologically adapted innate immunity.

Trem2 exists in both membrane-bound and soluble forms (sTrem2). In AD, sTrem2 promotes microglial survival via the PI3K/Akt pathway and enhances cytokine production through NF-κB signaling, independent of membrane Trem2 (16). In our study, the effects of sTrem2 were not validated in Trem2 KO mice. Thus, sTrem2 may act through Trem2 receptor-dependent mechanisms or via Trem2 receptor-independent pathways, which remains an important question for further investigation.

Microglial responses are more complex than the M1/M2 paradigm (7). Trem2 KO mice displayed expansion of IRMs subpopulation following PT-induced stroke (Fig. 4*B*). IRMs, linked to disease and cortical development (61, 62), can exacerbate inflammation through an aberrant IFN-I/cGAS/STING pathway thus hinders recovery after stroke (63), but may also support cortical remodeling and homeostasis (62). Therefore, increased IRMs in

Trem2 KO mice may reflect not only enhanced inflammation but also a shift toward reparative or homeostatic functions. DAM1 microglia exhibited a transitional profile with reduced homeostatic markers (Fig. 4*A* and *SI Appendix*, Fig. S9*A*). The predominant Spp1+ subpopulation corresponds to DAM2 microglia (Fig. 4*A* and *SI Appendix*, Fig. S9*A*), which play age-dependent roles in stroke (64). Trem2 depletion reduced Spp1+ DAM2 cells (Fig. 4*B*), supporting their detrimental role in stroke. In addition, MHC-II microglia, which exacerbate neurodegeneration (49), was reduced in Trem2 KO mice (Fig. 4*B*), and Gpnmb was identified as a marker of this subpopulation (Fig. 4*A* and *SI Appendix*, Fig. S9*A*), suggesting that Trem2 regulates MHC-II microglia through Gpnmb in ischemic stroke.

Integrative analysis of our RNA-seq data with patient-derived transcriptomic datasets identified Trem2 as a central regulator of stroke responses through multiple downstream targets. Although some candidates were not validated by qPCR, they may be differentially expressed in specific cell populations in Trem2 KO mice (Fig. 4*D* and *SI Appendix*, Fig. S9*E*). Ischemic stroke is characterized by dysregulated lipid metabolism closely linked to neuroinflammation (65). Notably, ABCA1, a key cholesterol transporter regulating lipid homeostasis (66) and ApoE metabolism in microglia (67), was altered. We also identified changes in lysosomal proteases cathepsin D (CTSD) and cathepsin Z. CTSD regulates ABCA1-mediated cholesterol efflux (68) and protects neurons from ischemic injury (69), implicating lysosomal dysfunction in Trem2-associated effects. Additionally, several Trem2-regulated genes associated with immune cell infiltration (70), including MILR1 (71), CD84 (72), and Siglec1 (73), suggesting that Trem2 coordinates crosstalk between resident microglia and infiltrating immune cells during stroke.

Gpnmb, originally described as an antitumor factor, can also promote immunosuppression in cancer (74, 75). Gpnmb depletion leads to reduced tumor growth and a shift toward a proinflammatory tumor microenvironment (76). In the central nervous system, Gpnmb is associated with anti-inflammatory and neurorepair functions (77). Its role in stroke appears to parallel that of Trem2: Previous MCAO studies reported modest (<2 fold) increases of Gpnmb (78, 79), whereas our PT model shows robust upregulation and detection of glycosylated isoforms, which may influence its function (*SI Appendix*, Fig. S11*A*). Like Gpnmb, Trem2 undergoes glycosylation, affecting trafficking and signaling (80, 81) (Fig. 1*H*). In vitro and in vivo studies demonstrate context-dependent roles for Gpnmb (82, 83), converging with Trem2 on PI3K/Akt and NF-κB pathways (16, 78, 79), highlighting the need for careful model selection.

Importantly, sGpnmb, like sTrem2, may serve as a biomarker. Both Trem2 and Gpnmb are cleaved by ADAM10 and released extracellularly (84, 85). Elevated serum sGpnmb have been associated with poor prognosis in cancers (86, 87), and both previous report and our findings in stroke patients align with these associations (79) (Fig. 6 *B*–*E*). Notably, recombinant sGpnmb ameliorates injury in the MCAO models (78), but exacerbates damage in our PT model (Fig. 5 *B*–*F*), underscoring model-dependent effects. However, larger patient cohorts are needed to establish clinical utility for sTrem2 and sGpnmb.

Our data show coordinated upregulation of Trem2 and Gpnmb at transcript and protein levels, suggesting synergistic roles in post-stroke neuroinflammation. Whether sGpnmb reversely modulates Trem2 or interacts with membrane-bound Gpnmb remains to be determined. Mapping the interactomes in ischemic conditions could reveal extracellular mechanisms and identify therapeutic targets to modulate microglial and immune responses. Our findings highlight that the pathophysiological role of a molecule may vary across experimental models, underscoring the importance of aligning model selection with clinical signatures to improve translational relevance.

Methods

Study Design. This study was designed to investigate the role of Trem2 in post-stroke neuroinflammation using a mouse model that closely replicates clinical conditions. Trem2 KO mice and sTrem2-injected mice were analyzed in a PT model. Cross-species analysis and experimental validation identified Gpnmb as a conserved Trem2 effector. This finding was further supported by analysis of plasma samples from stroke patients. Detailed methods are described in *SI Appendix*.

Data, Materials, and Software Availability. RNA-sequencing data have been deposited in GEO (GSE280846) (88). All other data are included in the manuscript and/or supporting information.

ACKNOWLEDGMENTS. We thank Dr. Marco Colonna (Washington University School of Medicine, St. Louis, MO) for providing the Trem2 KO mice. This study was supported by the National Natural Science Foundation of China (Nos. 32471009 to X.Z. and 32571141 to X.X.), Shenzhen Key Laboratory of Neuroimmunomodulation for Neurological Diseases (No. ZDSYS20220304163558001 to H.K.), Shenzhen Science and Technology Program (Nos. JCYJ20220818100803007 to X.Z. and JCYJ20210324120804012 to H.Z.), Shenzhen Science and Technology Program-The Excellent Youth Scholars (RCYX20221008092952129 to X.X.), Shenzhen Medical Academy of Research and Translation (A2303021 to X.X.), and Chinese Academy of Sciences Global Common Challenges Program (321GJHZ2023248GC to H.K.).

Author affiliations: [a]The Brain Cognition and Brain Disease Institute, Shenzhen Institutes of Advanced Technology, Chinese Academy of Sciences, Shenzhen 518055, China; [b]Bio-X international institute, Faculty of Life and Health Sciences, Shenzhen University of Advanced Technology, Shenzhen 518107, China; [c]Ministry of Education Key Laboratory of Gene Function and Regulation, Guangdong Province Key Laboratory of Pharmaceutical Functional Genes, State Key Laboratory of Biocontrol, School of Life Sciences, Sun Yat-sen University, Guangzhou 510275, China; [d]Shenzhen Key Laboratory of Neuroimmunomodulation for Neurological Diseases, Shenzhen 518055, China; [e]University of Chinese Academy of Sciences, Beijing 100049, China; [f]Shenzhen Hospital of Shanghai University of Traditional Chinese Medicine, Shenzhen 518001, China; [g]Luohu District Hospital of Traditional Chinese Medicine, Shenzhen 518001, China; [h]Max-Delbrück Center for Molecular Medicine, Berlin 13125, Germany; and [i]Shenzhen-Hong Kong Institute of Brain Science-Shenzhen Fundamental Research Institutions, Shenzhen 518055, China

1. GBDNSD Collaborators, Global, regional, and national burden of disorders affecting the nervous system, 1990–2021: A systematic analysis for the Global Burden of Disease Study 2021. *Lancet Neurol.* **23**, 344–381 (2024).
2. G. Tsivgoulis *et al.*, Thrombolysis for acute ischaemic stroke: Current status and future perspectives. *Lancet Neurol.* **22**, 418–429 (2023).
3. R. L. Jayaraj, S. Azimullah, R. Beiram, F. Y. Jalal, G. A. Rosenberg, Neuroinflammation: Friend and foe for ischemic stroke. *J. Neuroinflammation* **16**, 142 (2019).
4. X. Hu *et al.*, Microglial and macrophage polarization-new prospects for brain repair. *Nat. Rev. Neurol.* **11**, 56–64 (2015).
5. F. Leng, P. Edison, Neuroinflammation and microglial activation in Alzheimer disease: Where do we go from here? *Nat. Rev. Neurol.* **17**, 157–172 (2021).
6. U. K. Hanisch, H. Kettenmann, Microglia: Active sensor and versatile effector cells in the normal and pathologic brain. *Nat. Neurosci.* **10**, 1387–1394 (2007).
7. R. C. Paolicelli *et al.*, Microglia states and nomenclature: A field at its crossroads. *Neuron* **110**, 3458–3483 (2022).
8. R. Guerreiro *et al.*, TREM2 variants in Alzheimer's disease. *N. Engl. J. Med.* **368**, 117–127 (2013).
9. T. Jonsson *et al.*, Variant of TREM2 associated with the risk of Alzheimer's disease. *N. Engl. J. Med.* **368**, 107–116 (2013).
10. S. H. Lee *et al.*, Trem2 restrains the enhancement of tau accumulation and neurodegeneration by beta-amyloid pathology. *Neuron* **109**, 1283–1301 (2021).
11. C. Haass, Loss of TREM2 facilitates tau accumulation, spreading, and brain atrophy, but only in the presence of amyloid pathology. *Neuron* **109**, 1243–1245 (2021).
12. J. W. Lewcock *et al.*, Emerging microglia biology defines novel therapeutic approaches for Alzheimer's disease. *Neuron* **108**, 801–821 (2020).
13. T. R. Jay *et al.*, TREM2 deficiency eliminates TREM2+ inflammatory macrophages and ameliorates pathology in Alzheimer's disease mouse models. *J. Exp. Med.* **212**, 287–295 (2015).

14. C. E. G. Leyns *et al.*, TREM2 deficiency attenuates neuroinflammation and protects against neurodegeneration in a mouse model of tauopathy. *Proc. Natl. Acad. Sci. U.S.A.* **114**, 11524–11529 (2017).
15. F. A. Sayed *et al.*, Differential effects of partial and complete loss of TREM2 on microglial injury response and tauopathy. *Proc. Natl. Acad. Sci. U.S.A.* **115**, 10172–10177 (2018).
16. L. Zhong *et al.*, Soluble TREM2 induces inflammatory responses and enhances microglial survival. *J. Exp. Med.* **214**, 597–607 (2017).
17. X. Zhang *et al.*, Soluble TREM2 ameliorates tau phosphorylation and cognitive deficits through activating transgelin-2 in Alzheimer's disease. *Nat. Commun.* **14**, 6670 (2023).
18. M. Ewers *et al.*, Increased soluble TREM2 in cerebrospinal fluid is associated with reduced cognitive and clinical decline in Alzheimer's disease. *Sci. Transl. Med.* **11**, eaav6221 (2019).
19. E. Morenas-Rodriguez *et al.*, Soluble TREM2 in CSF and its association with other biomarkers and cognition in autosomal-dominant Alzheimer's disease: A longitudinal observational study. *Lancet Neurol.* **21**, 329–341 (2022).
20. M. Kawabori *et al.*, Triggering receptor expressed on myeloid cells 2 (TREM2) deficiency attenuates phagocytic activities of microglia and exacerbates ischemic damage in experimental stroke. *J. Neurosci.* **35**, 3384–3396 (2015).
21. R. Wu *et al.*, TREM2 protects against cerebral ischemia/reperfusion injury. *Mol. Brain* **10**, 20 (2017).
22. I. R. Turnbull *et al.*, Cutting edge: TREM-2 attenuates macrophage activation. *J. Immunol.* **177**, 3520–3524 (2006).
23. K. Kurisu *et al.*, Triggering receptor expressed on myeloid cells-2 expression in the brain is required for maximal phagocytic activity and improved neurological outcomes following experimental stroke. *J. Cereb. Blood Flow Metab.* **39**, 1906–1918 (2019).
24. M. W. Sieber *et al.*, Attenuated inflammatory response in triggering receptor expressed on myeloid cells 2 (TREM2) knock-out mice following stroke. *PLoS ONE* **8**, e52982 (2013).
25. T. Xue *et al.*, Sphingosine-1-phosphate, a novel TREM2 ligand, promotes microglial phagocytosis to protect against ischemic brain injury. *Acta Pharm. Sin. B* **12**, 1885–1898 (2022).
26. Q. Zhai *et al.*, Triggering receptor expressed on myeloid cells 2, a novel regulator of immunocyte phenotypes, confers neuroprotection by relieving neuroinflammation. *Anesthesiology* **127**, 98–110 (2017).
27. M. Maimaiti *et al.*, Blocking cGAS-STING pathway promotes post-stroke functional recovery in an extended treatment window via facilitating remyelination. *Med* **5**, 622–644 (2024).
28. Y. Guan *et al.*, Soluble TREM2 ameliorates pathological phenotypes in ischemic stroke models via modulating neuronal and microglial functions. *Exp. Brain Res.* **243**, 149 (2025).
29. H. S. Kwon *et al.*, Early increment of soluble triggering receptor expressed on myeloid cells 2 in plasma might be a predictor of poor outcome after ischemic stroke. *J. Clin. Neurosci.* **73**, 215–218 (2020).
30. G. Salafia *et al.*, Soluble Triggering Receptors Expressed on Myeloid cells (sTREM) in acute ischemic stroke: A potential pathway of sTREM-1 and sTREM-2 associated with disease severity. *Int. J. Mol. Sci.* **25**, 7611 (2024).
31. Y. Zhu *et al.*, The association between plasma soluble triggering receptor expressed on myeloid cells 2 and cognitive impairment after acute ischemic stroke. *J. Affect. Disord.* **299**, 287–293 (2022).
32. Y. Lu *et al.*, Soluble TREM2 is associated with death and cardiovascular events after acute ischemic stroke: An observational study from CATIS. *J. Neuroinflammation* **19**, 88 (2022).
33. M. L. Cotrina, N. Lou, J. Tome-Garcia, J. Goldman, M. Nedergaard, Direct comparison of microglial dynamics and inflammatory profile in photothrombotic and arterial occlusion evoked stroke. *Neuroscience* **343**, 483–494 (2017).
34. Y. Feng *et al.*, Infiltration and persistence of lymphocytes during late-stage cerebral ischemia in middle cerebral artery occlusion and photothrombotic stroke models. *J. Neuroinflammation* **14**, 248 (2017).
35. C. J. Price *et al.*, Intrinsic activated microglia map to the peri-infarct zone in the subacute phase of ischemic stroke. *Stroke* **37**, 1749–1753 (2006).
36. L. Ramiro *et al.*, Integrative multi-omics analysis to characterize human brain ischemia. *Mol. Neurobiol.* **58**, 4107–4121 (2021).
37. H. B. Huttner *et al.*, The age and genomic integrity of neurons after cortical stroke in humans. *Nat. Neurosci.* **17**, 801–803 (2014).
38. F. Betto, L. Chiricosta, E. Mazzon, An in silico analysis reveals sustained upregulation of neuroprotective genes in the post-stroke human brain. *Brain Sci.* **13**, 986 (2023).
39. B. Stamova *et al.*, Gene expression in peripheral immune cells following cardioembolic stroke is sexually dimorphic. *PLoS ONE* **9**, e102550 (2014).
40. T. Krug *et al.*, TTC7B emerges as a novel risk factor for ischemic stroke through the convergence of several genome-wide approaches. *J. Cereb. Blood Flow Metab.* **32**, 1061–1072 (2012).
41. D. M. Wu *et al.*, Immune pathway activation in neurons triggers neural damage after stroke. *Cell Rep.* **42**, 113368 (2023).
42. B. Han *et al.*, Integrating spatial and single-cell transcriptomics to characterize the molecular and cellular architecture of the ischemic mouse brain. *Sci. Transl. Med.* **16**, eadg1323 (2024).
43. L. M. Carey, D. F. Abbott, G. F. Egan, J. Bernhardt, G. A. Donnan, Motor impairment and recovery in the upper limb after stroke: Behavioral and neuroanatomical correlates. *Stroke* **36**, 625–629 (2005).
44. Q. Marlier, S. Verteneuil, R. Vandenbosch, B. Malgrange, Mechanisms and functional significance of stroke-induced neurogenesis. *Front. Neurosci.* **9**, 458 (2015).
45. G. Llovera, S. Roth, N. Plesnila, R. Veltkamp, A. Liesz, Modeling stroke in mice: Permanent coagulation of the distal middle cerebral artery. *J. Vis. Exp.* **89**, e51729 (2014).
46. B. Becher, S. Spath, J. Goverman, Cytokine networks in neuroinflammation. *Nat. Rev. Immunol.* **17**, 49–59 (2017).
47. S. Wang *et al.*, TREM2 drives microglia response to amyloid-beta via SYK-dependent and -independent pathways. *Cell* **185**, 4153–4169 (2022).
48. A. Stokowska *et al.*, Complement C3a treatment accelerates recovery after stroke via modulation of astrocyte reactivity and cortical connectivity. *J. Clin. Invest.* **133**, e162253 (2023).
49. Y. Chen, M. Colonna, Microglia in Alzheimer's disease at single-cell level. Are there common patterns in humans and mice? *J. Exp. Med.* **218**, e20202717 (2021).
50. S. Kedia *et al.*, T cell–mediated microglial activation triggers myelin pathology in a mouse model of amyloidosis. *Nat. Neurosci.* **27**, 1468–1474 (2024).
51. A. McQuade *et al.*, Gene expression and functional deficits underlie TREM2-knockout microglia responses in human models of Alzheimer's disease. *Nat. Commun.* **11**, 5370 (2020).
52. R. Sun *et al.*, TREM2 inhibition triggers antitumor cell activity of myeloid cells in glioblastoma. *Sci. Adv.* **9**, eade3559 (2023).
53. M. T. Patterson *et al.*, Trem2 promotes foamy macrophage lipid uptake and survival in atherosclerosis. *Nat. Cardiovasc. Res.* **2**, 1015–1031 (2023).
54. C. Wang *et al.*, Glycoprotein non-metastatic melanoma protein B functions with growth factor signaling to induce tumorigenesis through its serine phosphorylation. *Cancer Sci.* **112**, 4187–4197 (2021).
55. X. M. Gong *et al.*, Gpnmb secreted from liver promotes lipogenesis in white adipose tissue and aggravates obesity and insulin resistance. *Nat. Metab.* **1**, 570–583 (2019).
56. D. W. Simon *et al.*, The far-reaching scope of neuroinflammation after traumatic brain injury. *Nat. Rev. Neurol.* **13**, 171–191 (2017).
57. F. Bright *et al.*, Neuroinflammation in frontotemporal dementia. *Nat. Rev. Neurol.* **15**, 540–555 (2019).
58. H. Konishi, H. Kiyama, Microglial TREM2/DAP12 signaling: A double-edged sword in neural diseases. *Front. Cell Neurosci.* **12**, 206 (2018).
59. K. Schlepckow, E. Morenas-Rodriguez, S. Hong, C. Haass, Stimulation of TREM2 with agonistic antibodies-an emerging therapeutic option for Alzheimer's disease. *Lancet Neurol.* **22**, 1048–1060 (2023).
60. T. K. Ulland, M. Colonna, TREM2–A key player in microglial biology and Alzheimer disease. *Nat. Rev. Neurol.* **14**, 667–675 (2018).
61. J. P. Lopez-Atalaya, A. M. Bhojwani-Cabrera, Type I interferon signalling and interferon-responsive microglia in health and disease. *FEBS J.* **292**, 5921–5940 (2025).
62. C. C. Escoubas *et al.*, Type-I-interferon-responsive microglia shape cortical development and behavior. *Cell* **187**, 1936–1954 (2024).
63. P. Cui, B. Song, Z. Xia, Y. Xu, Type i interferon signalling and ischemic stroke: Mechanisms and therapeutic potentials. *Transl. Stroke Res.* **16**, 962–974 (2025).
64. Y. Lan *et al.*, Fate mapping of Spp1 expression reveals age-dependent plasticity of disease-associated microglia-like cells after brain injury. *Immunity* **57**, 349–363 (2024).
65. N. Bernoud-Hubac, A. Lo, A. N. Lazar, M. Lagarde, Ischemic brain injury: Involvement of lipids in the pathophysiology of stroke and therapeutic strategies. *Antioxidants* **13**, 634 (2024).
66. E. Boadu, R. C. Nelson, G. A. Francis, ABCA1-dependent mobilization of lysosomal cholesterol requires functional Niemann-Pick C2 but not Niemann-Pick C1 protein. *Biochim. Biophys. Acta* **1821**, 396–404 (2012).
67. V. Hirsch-Reinshagen *et al.*, Deficiency of ABCA1 impairs apolipoprotein E metabolism in brain. *J. Biol. Chem.* **279**, 41197–41207 (2004).
68. B. Haidar *et al.*, Cathepsin D, a lysosomal protease, regulates ABCA1-mediated lipid efflux. *J. Biol. Chem.* **281**, 39971–39981 (2006).
69. M. I. Hossain *et al.*, Restoration of CTSD (cathepsin D) and lysosomal function in stroke is neuroprotective. *Autophagy* **17**, 1330–1348 (2021).
70. Z. Jian *et al.*, The involvement and therapy target of immune cells after ischemic stroke. *Front. Immunol.* **10**, 2167 (2019).
71. K. Nanatsue *et al.*, Influence of MILR1 promoter polymorphism on expression levels and the phenotype of atopy. *J. Hum. Genet.* **59**, 480–483 (2014).
72. J. Sintes, X. Romero, J. de Salort, C. Terhorst, P. Engel, Mouse CD84 is a pan-leukocyte cell-surface molecule that modulates LPS-induced cytokine secretion by macrophages. *J. Leukoc. Biol.* **88**, 687–697 (2010).
73. R. M. Clancy *et al.*, Siglec-1 macrophages and the contribution of IFN to the development of autoimmune congenital heart block. *J. Immunol.* **202**, 48–55 (2019).
74. A. M. Lazaratos, M. G. Annis, P. M. Siegel, GPNMB: A potent inducer of immunosuppression in cancer. *Oncogene* **41**, 4573–4590 (2022).
75. M. Saade, G. Araujo de Souza, C. Scavone, P. F. Kinoshita, The role of GPNMB in inflammation. *Front. Immunol.* **12**, 674739 (2021).
76. F. Yalcin *et al.*, Tumor associated microglia/macrophages utilize GPNMB to promote tumor growth and alter immune cell infiltration in glioma. *Acta Neuropathol. Commun.* **12**, 50 (2024).
77. K. M. Budge, M. L. Neal, J. R. Richardson, F. F. Safadi, Glycoprotein NMB: An emerging role in neurodegenerative disease. *Mol. Neurobiol.* **55**, 5167–5176 (2018).
78. Y. Nakano *et al.*, Glycoprotein nonmetastatic melanoma protein B (GPNMB) as a novel neuroprotective factor in cerebral ischemia-reperfusion injury. *Neuroscience* **277**, 123–131 (2014).
79. Y. Ping *et al.*, GPNMB attenuates neuroinflammation and improves ischemic stroke via modulation of PI3K/Akt and p38 MAPK signaling pathways. *Brain Res.* **1849**, 149381 (2025).
80. K. Shirotani, D. Hatta, N. Wakita, K. Watanabe, N. Iwata, The role of TREM2 N-glycans in trafficking to the cell surface and signal transduction of TREM2. *J. Biochem.* **172**, 347–353 (2022).
81. J. S. Park, I. J. Ji, D. H. Kim, H. J. An, S. Y. Yoon, The alzheimer's disease-associated R47H variant of TREM2 has an altered glycosylation pattern and protein stability. *Front. Neurosci.* **10**, 618 (2016).
82. T. Li *et al.*, GPNMB ameliorates neuroinflammation via the modulation of AMPK/NFkappaB signaling pathway after SAH in mice. *J. Neuroimmune Pharm.* **18**, 628–639 (2023).
83. F. Shi *et al.*, Induction of matrix metalloproteinase-3 (MMP-3) expression in the microglia by lipopolysaccharide (LPS) via upregulation of glycoprotein nonmetastatic melanoma B (GPNMB) expression. *J. Mol. Neurosci.* **54**, 234–242 (2014).
84. A. A. Rose *et al.*, ADAM10 releases a soluble form of the GPNMB/Osteoactivin extracellular domain with angiogenic properties. *PLoS ONE* **5**, e12093 (2010).
85. G. Kleinberger *et al.*, TREM2 mutations implicated in neurodegeneration impair cell surface transport and phagocytosis. *Sci. Transl. Med.* **6**, 243ra286 (2014).
86. X. Feng *et al.*, High expression of GPNMB indicates an unfavorable prognosis in glioma: Combination of data from the GEO and CGGA databases and validation in tissue microarray. *Oncol. Lett.* **20**, 2356–2368 (2020).
87. Y. H. Huang *et al.*, Expression pattern and prognostic impact of glycoprotein non-metastatic B (GPNMB) in triple-negative breast cancer. *Sci. Rep.* **11**, 12171 (2021).
88. K. Li, S. Liu, X. Xiang, X. Zhu, Data from "Effects of Trem2 depletion on gene expressions in a mouse photothrombotic stroke model." Gene Expression Omnibus (GEO). https://www.ncbi.nlm.nih.gov/geo/query/acc.cgi?acc=GSE280846. Deposited 1 November 2024.